

# BOND STRESS-SLIP BEHAVIOR OF STEEL FIBERS EMBEDDED IN ULTRA HIGH PERFORMANCE CONCRETE

K. Wille<sup>1</sup> and A. E. Naaman<sup>2</sup>

<sup>1</sup>University of Connecticut, CEE Department, 261 Glenbrook Road,  
Storrs, Connecticut 06269-2037, USA  
(formerly Postdoc at University of Michigan)

<sup>2</sup>University of Michigan, CEE Department, 2340 G.G. Brown,  
Ann Arbor, Michigan 48109-2125, USA

## ABSTRACT

This research work focuses on the pull-out behavior of high strength straight smooth steel fibers embedded in ultra high performance concretes (UHPC). The UHPCs used were designed to achieve a compressive strength of about 200 MPa (29 ksi) without recourse to heat treatment or pressure curing. The high particle packing density of UHPCs provides high physico-chemical bond between fiber and matrix. This leads to an unexpected phenomenological bond-slip-hardening behavior for straight smooth brass-coated steel fibers, commonly used in ultra high performance fiber reinforced concretes (UHP-FRC). Such slip-hardening bond was so far not encountered with normal strength concrete matrices. Microscopical studies revealed one reason for this phenomenon that is, scratching of the brass-coated fiber surface by the fine sand and abrading matrix particles. It was observed that not only the matrix compressive strength influences significantly the bond behavior, but also for a given compressive strength the matrix composition plays a major role. By optimizing both the compressive strength and the composition of the matrix, equivalent bond strengths exceeding 20 MPa were achieved.

## KEYWORDS

pull out, UHPC, bond slip hardening, high strength steel fiber,

## INTRODUCTION

Some of the most promising cementitious materials in construction applications are high performance fiber reinforced cementitious composites (HP-FRCC). Their ability to achieve a post-cracking tensile strength higher than the matrix tensile strength results in strain hardening tensile behavior and in the development of multiple cracking. This characteristic is particularly suitable for the design of structural elements with high energy absorption properties. Further improvements in these properties can be achieved through an increase in matrix strength and/or an improvement in the bond at the fiber-matrix interface leading to ultra high performance fiber reinforced concrete (UHP-FRC). Note that in order to obtain strain-hardening behavior with comparable fiber volume fractions, an increase in the matrix tensile strength requires a simultaneous improvement in the bond between fiber and matrix. Single fiber pull-out tests provide basic information on the interfacial properties between fiber and matrix and allow for optimizing the bond stress versus slip behavior, which influences the tensile properties of the composite.

The pull out behavior of single smooth, straight steel fibers embedded in normal and high strength concrete (HSC) has been investigated by numerous researchers, as briefly summarized in [1],[2]. Figure 1a shows a typical pull-out load versus slip relationship  $P(s)$  of

a smooth fiber embedded in a high strength concrete. After a quasi linear ascending branch, the load drops suddenly, indicating the completion of debonding along the fiber, followed by a steady load decrease due to the reduction of the embedment length. After debonding the pull out resistance is predominately based on friction between fiber and matrix.

The load at any slip  $s$ ,  $P(s)$ , divided by the current embedded lateral surface area of the fiber  $A_o(s) = \pi \times d_f \times (L_E - s)$  leads to the slip dependent shear stress  $\tau(s)$ , which is averaged over the current embedment length  $L_E - s$ , where  $L_E$  is the initial embedment length,  $s$  the slip during pull out and  $d_f$  the fiber diameter (Equation 1):

$$\tau(s) = \frac{P(s)}{\pi \times d_f \times (L_E - s)} \quad \text{in MPa (N/mm}^2\text{)} \quad (1)$$

The curve in Fig. 1b is derived based on that of Fig. 1a, using Eq. (1); it shows the shear stress-slip relationship with a maximum shear stress of  $\tau_{\max} = 3.2$  MPa at the peak point, and a practically constant shear stress after debonding of  $\tau_f = 1.2$  MPa, which illustrates the action of a constant frictional bond.

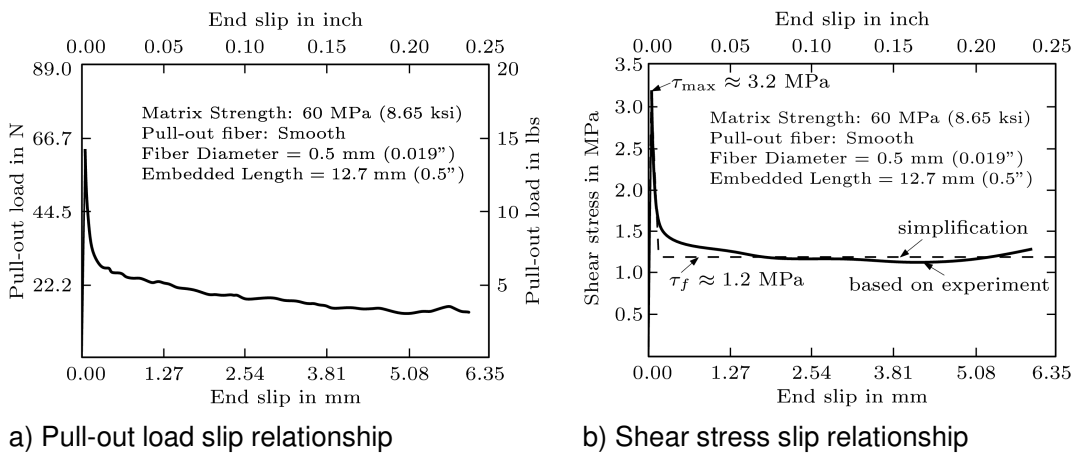


**Fig. 1:** Pull-out behaviour of straight steel fibers embedded in high strength concrete (HSC) according to Naaman and Najm 1991 [1]

In comparison to research conducted on the pull out behavior of steel fibers embedded in normal and high strength cementitious matrices, little information can be found so far on the bond behavior of high strength straight smooth steel fibers ( $d_f \approx 0.2$  mm) pulled out from an ultra high strength matrix, UHPC [2-5]. Although the increased compressive strength of the matrix results in higher bond strength, chemical treatment of the fiber surface [2] such as based on phosphatation [6] or mechanical fiber surface treatment through scratching with sand paper [5] have been investigated to increase fiber efficiency.

In ultra-high performance fiber reinforced cement (UHP-FRC) composites, smooth straight steel fibers with tensile strengths often exceeding 3000 MPa, and diameters as small as 0.12 mm, are used. Such steel fibers are often brass or zinc coated to facilitate production and improve corrosion resistance. The main goal of this research was to evaluate, understand and possibly improve the bond behavior of commercially available straight brass-coated high strength steel fibers embedded in UHPC matrices, with particular attention to tailoring the matrix mixture composition.

## EXPERIMENTAL PROGRAM AND TESTING

### Materials and mixture composition

One type of high strength steel fiber (S-fiber) was used throughout this study, with the following properties:  $\ell_f / d_f = 13/0.2$  mm, brass-coated, straight and smooth, high tensile strength ( $\sigma_f \approx 2600$  MPa). The fibers were embedded in nine different ultra high performance concretes (UHPC) mixtures whose composition is summarized in Table 1. Note that the matrices include an ultra high performance paste (UHPP), consisting of cement (C), silica fume (SF), glass powder (GP), water (W) and superplasticizer (SPL), that is, without sand of larger particle size. Detailed information on the mix design of these UHPC mixtures is provided in [7]. Their compressive strength (without fibers) ranged from 194 MPa to 240 MPa, and was achieved by paste optimization without using heat, pressure or other special treatments. Despite their low water to cement ratio of  $W/C \approx 0.2$ , they exhibited a high workability (see  $d_{sp}$  values in Table 1) with self-consolidating characteristics; this is particularly important to increase the consistency of the test results and mitigate the influence of compaction by vibration.

The parameters to be investigated included the influence of the amount and hardness of sand, the dispersion efficiency of small particles and the median particle size of silica fume on the pull-out bond behavior of a single embedded steel fiber. In Table 1, the second row identifying a mixture illustrates the main parameter to be evaluated; so the mixture with SPL-A differs from that with SPL-B by its type of superplasticizer; other mixtures show the type and or proportions of sands, and silica fume. A microscopic study was also carried out to better understand the reasons for the atypical bond-slip hardening behavior of S-fibers pulled out of UHPC matrices.

Type	UHPP	UHPC SPL-A	UHPC SPL-B	UHPC 0/100	UHPC 30/70	UHPC 50/50	UHPC 100/0	UHPC Zircon	UHPC SF-B
C	1	1	1	1	1	1	1	1	1
SF	0.25 <sup>a</sup>	0.25 <sup>b</sup>							
GP	0.25	0.25	0.25	0.25	0.25	0.25	0.25	0.25	0.25
W <sup>c</sup>	0.21	0.22	0.195	0.195	0.195	0.195	0.203	0.199	0.195
SPL <sup>d</sup>	0.0072 <sup>e</sup>	0.0054 <sup>e</sup>	0.0108 <sup>f</sup>	0.0108 <sup>f</sup>	0.0108 <sup>f</sup>	0.0108 <sup>f</sup>	0.0142 <sup>f</sup>	0.0125 <sup>f</sup>	0.0108 <sup>f</sup>
Sand A <sup>g</sup>	0	0.28	0.2	0	0.3	0.5	1	1.75 <sup>h</sup>	0.3
Sand B <sup>i</sup>	0	1.1	0.81	1	0.71	0.5	0	0	0.71
Sand A/B	0/0	20/80	20/80	0/100	30/70	50/50	100/0	100/0	30/70
$f_c$ (MPa) <sup>j</sup>	229	194	197	196	207	210	212	201	240
$d_{sp}$ (mm) <sup>k</sup>	322	296	294	293	304	292	263	272	320

<sup>a</sup> silica fume type A ( $d_{50} = 1.2 \mu\text{m}$ ); <sup>b</sup> silica fume type B ( $d_{50} = 0.5 \mu\text{m}$ ); <sup>c</sup> total water; <sup>d</sup> solid content; <sup>e</sup> superplasticizer type A; <sup>f</sup> superplasticizer type B; <sup>g</sup> silica sand  $d_{\text{max}} = 0.2$  mm; <sup>h</sup> zircon sand ( $\text{ZrSiO}_4$ )  $d_{\text{max}} = 0.2$  mm; <sup>i</sup> silica sand  $d_{\text{max}} = 0.8$  mm; <sup>j</sup> concrete age 28 days, specimen geometry cube ( $a = 50$  mm); <sup>k</sup> spread value on flow table in accordance with ASTM C 230/ C 230M; <sup>l</sup> based on brass-coated single fiber pull-out tests with  $d_f = 0.2$  mm and  $L_E = 6.4$  mm

**Table 1:** Mixture proportions by weight of the UHPP and UHPC matrices investigated

### Specimen preparation

All ingredients for each matrix were mixed together in a small paddle mixer following the mixing procedure recommended in [7], which takes on average 16 minutes. After mixing, the self consolidating mixture was poured without vibration in half dogbone-shaped molds each surrounding one single fiber, which was carefully aligned and held in place by a piece of hard foam (Fig. 2). After casting, the specimens were covered with plastic sheets and stored at

room temperature for 24 hours. Then they were removed from their molds and stored in a water tank at 20°C for an additional 26 days prior to testing. All specimens were tested at an age of 28-29 days that is in a dry condition after kept in air for a minimum of 24 hours.

### Test setup

The half dogbone-shaped specimens were placed in a test fixture (Fig. 2), which allowed centering and holding the specimen in place without applying additional lateral pressure on the fiber. After positioning and centering, the fiber is tightly gripped within the fixture which is attached to the load cell (max. 500 lbs) of an MTS deformation controlled servo-hydraulic testing machine. The vertical deformation of the grip system, defined as fiber slip, was measured by an attached LVDT. Elastic deformation of the fiber and the specimen was neglected in the presentation of the results.

As recommended in [8], the pullout load speed was set to  $v = 0.018$  mm/s. The fibre embedment length was targeted to  $L_E = 6.5$  mm that is half the length of the fiber used. The actual embedded length was measured more exactly after complete fiber pull-out.

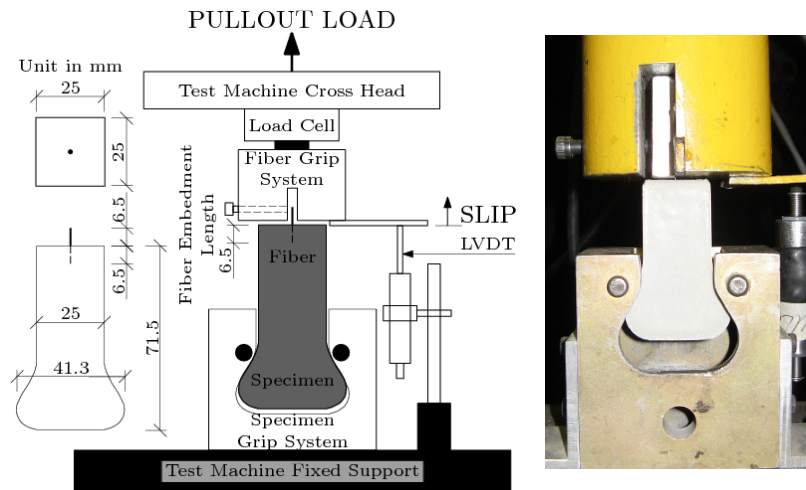


Fig. 2: Pull out specimen and test setup, according to [8]

For each matrix, a series consisting of 5 specimens was tested. All displayed experimental results represent the calculated average curve of each series based on the test results of 5 specimens.

## EXPERIMENTAL AND ANALYTICAL RESULTS

### Influence of sand and the dispersion of small particles

The pull-out load versus slip behavior of S-fiber embedded in UHPC SPL-A is plotted in Fig. 3a; it differs significantly from the pull-out behavior of a smooth fiber embedded in HSC (Fig. 1a). Instead of showing a drastic drop after reaching the maximum load, the pull-out resistance steadily decreases and drops only shortly before the fiber is completely pulled out. The calculated shear stress at peak load for the UHPC SPL-A series is  $\tau \approx 6$  MPa about twice that observed for the high strength concrete matrix (Fig. 1b). Moreover, unlike what is observed for HSC (Fig. 2b) where an almost constant frictional stress develops, the fiber shear stress in UHPC steadily increases with an increase in fiber slip (Fig. 3b). This characteristic was observed for all the series tested except the one without sand that is UHPP. The results of Fig. 3b for series SPL-A and SPL-B lead to the conclusion that the

frictional bond of the debonded fiber also increases until the fiber is completely pulled out. Therefore the frictional coefficient  $\mu$  and/or the fiber surface pressure  $\sigma_N$  must have increased.

Chan and Chu [3] investigated the influence of silica fume on the pull out behavior of steel fibers embedded in reactive powder concrete (RPC). Microscopical analysis revealed some adhesion of matrix particles to the fiber surface, most significant when the silica fume content was between 20 % and 30 % of cement by weight; that is very similar to the UHPCs in this study. It is possible that the abrasion of these particles and their accumulation towards the fiber pull out end might cause a wedge effect leading to higher pressure on the fiber and higher frictional bond. Based on the pull-out load slip relationship given in [3] for a fiber group of 9 fibers and considering the higher embedment length of 10 mm, the shear stress slip relationship was calculated and confirms the shear stress behavior observed in this research. The corresponding curve is shown in Fig. 3b as a dotted line and compares well with the curves obtained in this study. Note that the better performance shown in Fig. 3 by UHPC-SPL B compared to UHPC-SPL A may be explained by the better dispersion of glass powder and silica fume observed when SPL B was used.

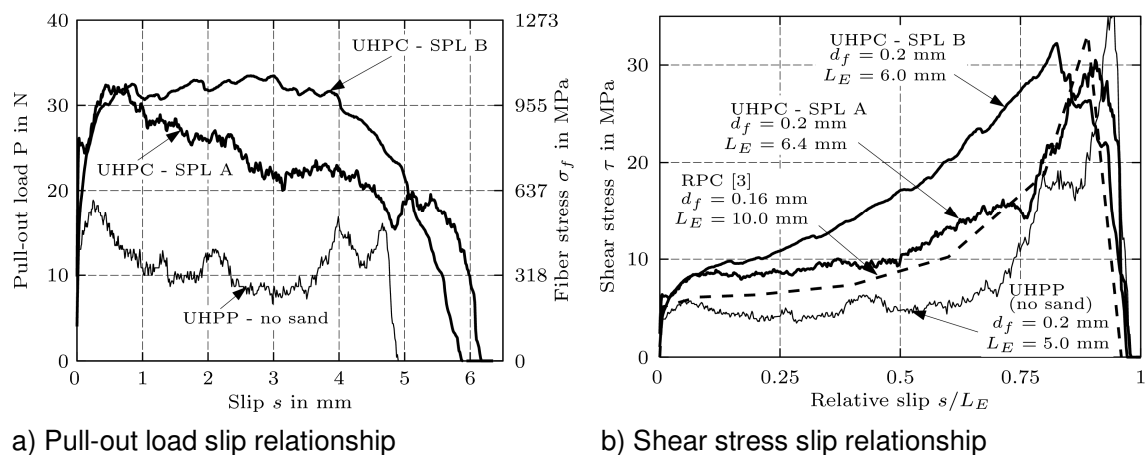


**Fig. 3:** Influence of silica sand and superplasticizer on the pull-out behavior

Also Chan and Wu [3] reported that longitudinal scratches on the fiber surface were microscopically observed. Similar scratches were observed in this research (Fig. 4b), which suggests an increase in the frictional coefficient and improved bond. Moreover, it is noted that the plastic deformation of the fiber end due to the cutting process provides some mechanical anchorage (Fig. 4c), which also may help increasing the pull-out resistance; its effect is especially noticeable just before the complete fiber pull-out. In summary the following three effects should be assessed to explain the bond-slip hardening behavior of smooth steel fibers: 1) wedge effect of the abraded particles, 2) scratching of the fiber surface, and 3) fiber end deformation.

Referring back to Fig. 3b, it can be observed that the fiber shear resistance in UHPP was not only significant lower than the two others, but also showed a shear stress hardening only at the end of the fiber pull-out. This result was surprising since the compressive strength of UHPP was 229 MPa, about 20 % higher than UHPC SPL-A, and was expected to offer a higher fiber surface pressure due to higher shrinkage. However, no fiber scratching could be observed (Fig. 4a) in this fiber, suggesting that the bond hardening at the end of the curve in Fig. 3b was due mostly to the mechanical influence of the cut end of the fiber. This leads to the conclusion that sand, present in UHPC SPL-A and SPL-B, may significantly influence the roughness of the tunnel of matrix surrounding the fiber in order to scratch the fiber and increase the frictional component.

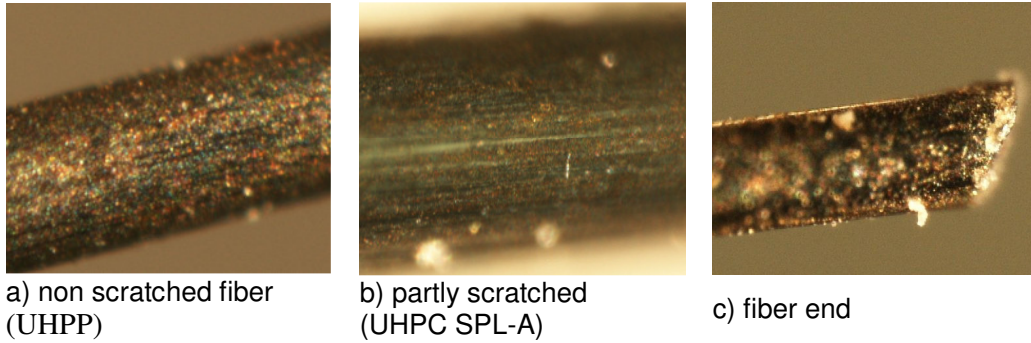


Fig. 4: Stereomicroscopical evaluation of the effect of scratching of the brass coating in steel fibers embedded in UHPC

In a prior study [9], in order to improve the dispersion of small particles like silica fume and glass powder a more efficient superplasticizer (SPL-B) was selected and incorporated in the mix design. Its efficiency was evaluated by its ability to reduce the  $W/C$  ratio without reducing the spread  $d_{sp}$  (see Table 1) of the flow cone test. The use of SPL-B led not only to a slight increase in compressive strength (Table 1) but also a higher pull-out load and shear stress resistance at large slips (Fig. 3). This indicates a higher frictional bond, presumably caused by a larger amount of particles adhering to the fiber surface and abraded during fiber pull-out. Indeed, damage on the fiber surface after pull-out was observed microscopically.

Besides the mixture for UHPC SPL-B, characterized by Sand A ( $d_{max} = 0.2$  mm) to Sand B ( $d_{max} = 0.8$  mm) ratio of 20/80, mixtures with different Sand A to Sand B ratios were also investigated in order to evaluate the influence of sand on the bond behavior. Figure 5a illustrates the pull-out load versus slip results observed and why mixture SPL-B was selected. Although a slightly higher compressive strength was achieved by changing the Sand A/B ratio from 0/100 to 100/0 (Table 1) the bond behavior remained practically unchanged (Fig. 5), except for the lower performance of the fiber embedded in UHPC 0/100 (no fine Sand A present).

Based on the median particle size of  $d_{50,SAND A} = 0.11$  mm and  $d_{50,SAND B} = 0.5$  mm and the assumption of an ideal spherical shape, there are 94 times more particles of Sand A than Sand B in the mix of UHPC 50/50 and 23 times more particles of Sand A than Sand B in UHPC 20/80. This may explain why similar shear stress slip relationships of the fibers embedded in UHPC 20/80, 30/70, 50/50 and 100/0 are observed.

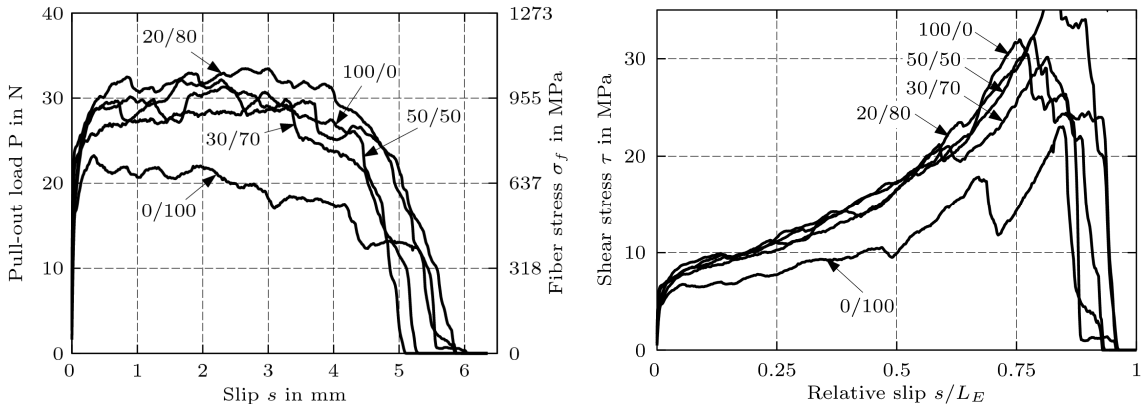


Fig. 5: Influence of the ratio of silica Sand A and Sand B on the pull-out behaviour

### Influence of Mohs' hardness of sand and finesse of silica fume on the fiber surface damage

Given an ultra high performance matrix, the aforementioned results have shown that silica sand plays an important role in scratching the brass-coated steel fiber surface, thus improving frictional bond. The ability to scratch other materials can be evaluated by Mohs' hardness, a scale ranging from 0 (softest) to 10 (hardest). Tabor [10] physically interpreted Mohs' hardness scale and found a linear logarithmic relationship between the indentation hardness ( $H$ ) and Mohs' hardness ( $M$ ) as follows:

$$\log(H) = n \times M + k \quad (2)$$

where  $n \approx \log(1.6) = 0.204$  and  $k \approx 1.495$ . Therefore an increase in  $M$  by 1 represents an increase in  $H$  by 60 %.

Tabor [10] also stated that at least a 20 % higher indentation hardness of a given material is required to scratch the softer material. Given this condition the following equation can be derived from Eq. (2):

$$\Delta M_{scratch} = \frac{\log(1.2)}{\log(1.6)} = \log_{1.6}(1.2) = 0.39 \quad (3)$$

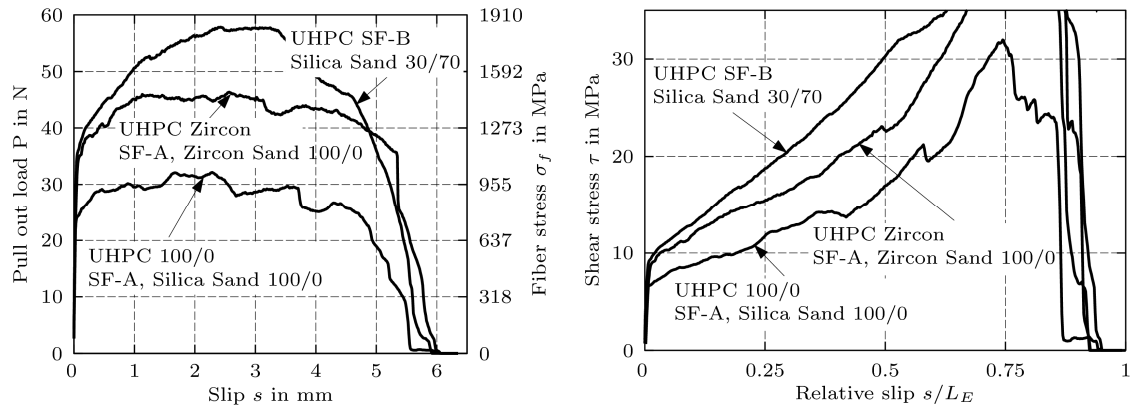
Hence, for practical purposes, a material is able to scratch another one, if its Mohs' hardness is higher by about 0.4. Silica sand, which consists of 99.8 % silicon dioxide ( $\text{SiO}_2$ ), is characterized by a Mohs' hardness of up to 7; it is thus able to scratch brass with a Mohs' hardness  $M \approx 3.5$  used as coating for the high strength steel fiber investigated in this research. With a given value of Mohs' hardness of  $M \approx 7$  to 8 for hardened steel, silica sand should not be able to scratch the steel under the brass-coating.

	Brass Cu&Zn	Silica sand SiO <sub>2</sub>	Zircon sand ZrSiO <sub>4</sub>	hardened steel
Mohs' hardness	3.5	7	7.5	7-8

Table 3: Mohs hardness for different materials

An attempt was made to use a zircon sand which exhibits a higher Mohs' hardness ( $M \approx 7.5$ ) in order to increase the possibility to scratch the steel under the brass-coating. Its use (UHPC Zircon) did not adversely influence the fresh mix properties based on UHPC 100/0 (silica sand was replaced by an equal volume of zircon sand) (Table 1).

The pull-out behaviors of S-fibers embedded in UHPC Zircon showed a remarkable increase in the maximum load (30 %) as well as in bond slip hardening (Fig. 6). The surface of the pulled out fiber was significantly damaged and longitudinally scratched. Clearly the zircon sand was harder on the brass coating. Although the scratching seemed to be different from the specimens previously observed, it was not clear whether the steel under the brass-coating had been scratched or not.



a) Pull-out load slip relationship

b) Shear stress slip relationship

**Fig. 6:** Influence of sand Mohs' hardness (silica sand: approx. 7, zircon sand: 7.5) and the fineness of silica fume (SF-A:  $d_{50} = 1.2 \mu\text{m}$ , SF-B:  $d_{50} = 0.5 \mu\text{m}$ ) on the pull-out behaviour

Further enhancement in the pull-out behavior was achieved when using a different type of silica fume (SF-B), characterized by a smaller mean particle size of  $d_{50} = 0.5 \mu\text{m}$  in comparison to SF-A ( $d_{50} = 1.2 \mu\text{m}$ ). SF-B was incorporated in the mix design of UHPC SF-B without adversely affecting the workability of the mix, leading to a compressive strength of 240 MPa under laboratory conditions, without special treatment. In comparison to UHPC Zircon another increase of 25 % in the maximum pull out load was achieved and an improved stress-slip hardening behavior calculated. The reason for this behavior can be explained by the intensively damaged fiber surface. The brass coating was not only scratched but in most cases completely delaminated from the steel surface. This was observed on the surface of pulled out fibers (Fig. 7b), on the surface of the tunnel of matrix left after fiber pull-out (Fig. 7c), and also on the failure surface of tested tensile specimens made out of ultra high strength fiber reinforced concrete (UHP-FRC) based on the mix design of UHPC SF-B.

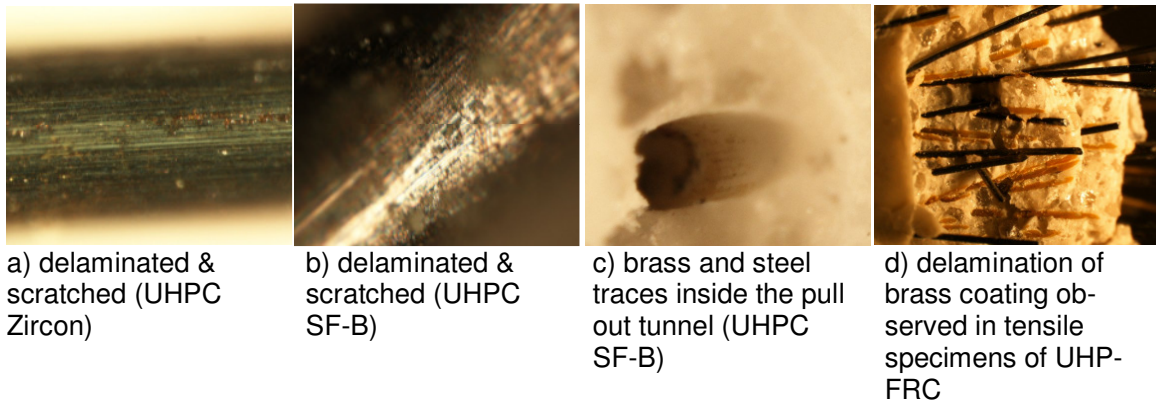


**Fig. 7:** Stereo-microscopical study to visualize the effects of delamination and scratching of brass-coated fibers embedded in UHPC with optimized interfacial properties

## RESULTS COMPARISON

The maximum tensile stress induced in the fiber by the maximum pull-out load can be calculated from:

$$\sigma_{\max} = \frac{P_{\max}}{A_f} \quad \text{in MPa (N/mm}^2\text{)} \quad (4)$$

where  $A_f$  is the cross sectional area of the fiber. It is a good measure of the utilization of the fiber material. Another measure is the equivalent bond strength,  $\tau_{eq}$ , defined as the average bond strength based on the energy  $W_p$  dissipated during the entire fiber pull out:

$$\tau_{eq} = \frac{2 \times W_p}{\pi \times d_f \times L_E^2} \quad \text{in MPa (N/mm}^2\text{)} \quad (5)$$

where  $W_p$  is given by:

$$W_p = \int_{s=0}^{s=L_E} P(s) ds \quad \text{in Nmm (J} \times 10^{-3}\text{)} \quad (6)$$

The pull out work or energy  $W_p$ , defined by Equation (6) represents the area under the pull out load versus slip curve.

The unit pull out work or energy per embedded fiber surface area is termed  $w_p$  and defined by :

$$w_p = \frac{W_p}{\pi \times d_f \times L_E} \quad \text{in N/mm (J} \times 10^{-3}\text{/mm}^2\text{)} \quad (7)$$

In the pull-out load curves described in Figs. 3, 5 and 6, the maximum load occurs at different slips. To simplify the comparison between different series,  $\tau_{av}$  is defined as the average bond strength based on the maximum pull-out load and the initial embedment length and is given by:

$$\tau_{av} = \frac{P_{\max}}{\pi \times d_f \times L_E} \quad \text{in MPa (N/mm}^2\text{)} \quad (8)$$

The values of  $P_{\max}$ ,  $\sigma_{\max}$ ,  $\tau_{av}$ ,  $\tau_{eq}$  and  $w_p$  are given in Table 3 for the ultra high performance matrices used in this research. These values should provide basic information for the analysis of the tensile behavior of UHP-FRC.

Figure 8 provides a visual rendition of the main results given in Table 3. It can be observed for instance that in comparison to HSC the stress induced in the fiber embedded in UHPC SPL-A is more than doubled, and almost quadrupled if the fiber is embedded in UHPC SF-B with an optimized interfacial bond (Fig. 8a). With an induced maximum fiber tensile stress  $\sigma_{\max} = 1841$  MPa the fiber material is utilized at 71 %. In terms of dissipated pull-out energy, represented by the values of equivalent bond strength or relative pull-out work the values follow the same trend for the different matrices as shown in Fig. 8b. In particular, UHPC SF-B gives a pull-out work value about 20 times that of HSC.

Type	UHPP	UHPC SPL-A	UHPC SPL-B	UHPC 0/100	UHPC 30/70	UHPC 50/50	UHPC 100/0	UHPC Zircon	UHPC SF-B
$P_{\max}$ (N) <sup>a</sup>	22.0	35.6	35.5	23.3	30.7	31.3	32.2	46.4	57.8
$\sigma_{\max}$ (MPa) <sup>a</sup>	709	1133	1130	740	978	997	1024	1476	1841
$\tau_{av}$ (MPa) <sup>a</sup>	5.5	8.9	8.8	5.8	7.6	7.8	8.0	11.5	14.4
$\tau_{eq}$ (MPa) <sup>a</sup>	6.1	10.4	14.3	11.6	13.3	14.5	13.5	19.4	22.1
$w_p$ (N/mm) <sup>a</sup>	19.5	33.3	45.9	37.0	42.5	46.3	43.2	62.1	70.7

<sup>a</sup> based on brass-coated single fiber pull-out tests with  $d_f = 0.2$  mm and  $L_E = 6.4$  mm

<sup>b</sup> for HSC:  $\sigma_{\max} = 430$  MPa,  $\tau_{av} = 3$  MPa,  $\tau_{eq} = 1$  MPa,

Table 3: Key pull-out results of single brass coated steel fiber embedded in UHPP and UHPC

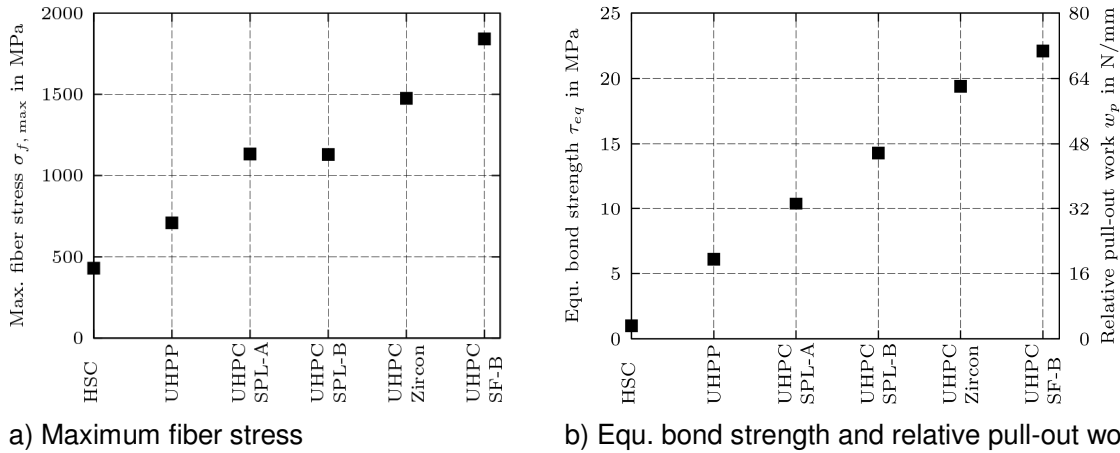


Fig. 8: Influence of different cementitious matrices on maximum fiber stress, equivalent bond strength and relative pull-out work based on brass-coated single fiber pull-out tests with  $d_f = 0.2$  mm and  $L_E = 6.4$  mm

Figure 9 is a plot of the data for maximum tensile stress induced in the fiber versus the compressive strength of the matrix used. It can be observed that a high compressive strength is a necessary, but not sufficient condition to achieve a very high fiber tensile stress during pull-out and thus, a high utilization factor of the fibers.

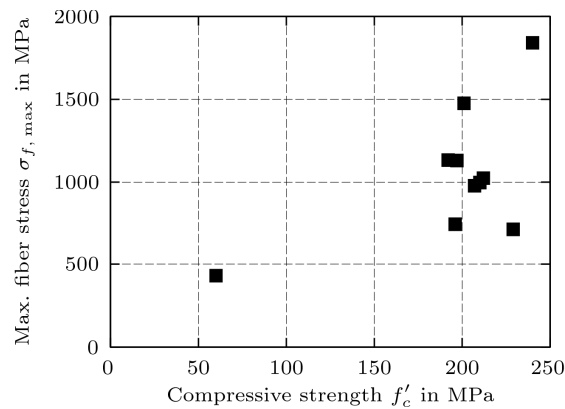


Fig. 9: Influence of compressive strength on the maximum fiber stress based on brass-coated single fiber pull-out tests with  $d_f = 0.2$  mm and  $L_E = 6.4$  mm

## CONCLUDING REMARKS

The research work described above focused on the pull-out behavior of high strength straight smooth steel fibers embedded in ultra high performance concretes (UHPC). These fibers are generally brass-coated and widely used in research studies and applications of UHP-FRCs. The UHPCs used had a compressive strength ranging from 194 MPa to 240 MPa, achieved by paste optimization and particle packing without resorting to heat, pressure or other special treatments. The fibers used in all the pull-out tests were brass-coated with a diameter of 0.2 mm.

The pull-out test results showed an un-expected hardening of the bond stress versus slip curve, unlike prior observations for the pull-out behavior of straight smooth steel fibers embedded in normal strength concrete. Microscopic analysis suggested that the three following effects may explain the bond-slip hardening behavior of smooth fibers: 1) wedge effect of adhered and abraded particles, 2) scratching of the fiber surface, and 3) fiber end deformation due to the cutting process.

Particular attention was placed on the improvement of the interfacial bond between fiber and cement matrix by improving the dispersion of small particles in the mix, the use of zircon sand with an increased hardness as well as the use of silica fume with a smaller mean particle size. As a result tensile stresses induced in the fibers (with an embedded length of about 6.5 mm) under pull-out reached up to 1841 MPa. Such values are at least four times higher than what is generally achieved with normal and high strength concrete. Similarly equivalent bond strength up to 20 MPa, and pull-out work or energy per unit embedded surface area of up to 71 N/mm were observed. Such pull-out work is up to 20 times that obtained with conventional and high strength concrete matrices. The results also demonstrate that a high compressive strength is a necessary, but not sufficient condition for achieving a very high equivalent bond strength.

It is believed that this investigation will help design UHP-FRC with significant tensile strength and strain-hardening behavior in tension, as well as significantly improved energy dissipation capacity.

## ACKNOWLEDGEMENTS

This research work was supported by a fellowship from the Postdoctoral-Programme of the German Academic Exchange Service (DAAD) and by the US National Science Foundation under grant No. CMS 0754505. The second author would also like to acknowledge prior support by the German Alexander von Humboldt Foundation which allowed him to establish research collaboration with German colleagues. The opinions expressed in this paper are those of the authors and do not necessarily reflect the views of the sponsors.

## REFERENCES

- [1] Naaman, A. E. and H. Najm:  
Bond-Slip Mechanisms of Steel Fibers in Concrete, in ACI Materials Journal, Vol. 88, No. 2, 1991, pp. 135-145.
- [2] Orange, G., Acker, P. and C. Vernet:  
A new generation of UHP concrete: DUCTAL damage resistance and micromechanical analysis, in proceedings of RILEM- High Performance Fiber Reinforced Cement Composites (HPFRCC3), edited by H. W. Reinhardt and A. E. Naaman, 1999, pp. 101-111.

- [3] Chan, Y.-W. and S.-H. Chu:  
Effect of silica fume on steel fiber bond characteristics in reactive powder concrete, in Cement and Concrete Research, Vol. 34, No. 7, 2004, pp. 1167–1172.
- [4] Markovic, I.:  
High-Performance Hybrid-Fibre Concrete – Development and Utilisation, Technische Universität Delft, Ph.D. thesis, 2006.
- [5] Stengel, T.:  
Effect of Surface Roughness on the Steel Fibre Bonding in Ultra High Performance Concrete (UHPC), in Proceedings of the NICOM3 (Nanotechnology in Construction 3), 2009
- [6] Sugama, T., Carciello, N., Kukacka, L. E. and G. Gray:  
Interface between zinc phosphate-deposited steel fibers and cement paste, Journal of Materials Science, Vol. 27, 1992, pp. 2863-2872.
- [7] Wille, K., Naaman, A. E. and G. J. Parra-Montesinos:  
Ultra high performance concrete with compressive strength exceeding 150 MPa (22 ksi): A simpler way, in ACI Materials Journal, 2009, accepted.
- [8] Kim, D., El-Tawil, S. and A. E. Naaman:  
Loading Rate Effect on Pullout Behavior of Deformed Steel Fibers, in ACI Materials Journal, 2008, pp. 576-584.
- [9] Wille, K., Naaman, A. E. and G. J. Parra-Montesinos:  
Ultra High Performance Concrete with Compressive Strength Exceeding 150 MPa (22 ksi): A Simpler Way, Department of Civil and Environmental Engineering, University of Michigan, 2009, 47 pp.
- [10] Tabor, D.:  
Mohs's Hardness Scale – A Physical Interpretation, in Proc. Phys. Soc. B 67 249, 1954, pp. 249-257.

**Corresponding author:** kwille@umich.edu